Control of Debris Flow Using Steel-grid SABO Dams

Norio HARADA[1,*] and Yoshifumi SATOFUKA[2]

[1] Dept. of Erosion Control Engineering, Mitsui Consultants Co., Ltd. (Benten, Minatoku, Osaka 5520007, Japan)

[2] Dept. of Civil, Ritsumeikan University (Noji, Kusatsu, Shiga 5258577, Japan)

*Corresponding author. E-mail: harada@mccnet.co.jp

Debris flows can be obstructed by common steel-grid SABO dams through the formation of a blockade of coarse woody debris, especially in the absence of large-diameter sand. A better understanding of the blockading mechanism would enable the development of more efficient dam structures. The permeable width of the barricade is determined by the maximum particle diameter D_{95}, not the grain-size distribution. To optimize dam structure, accurate information about the grain-size distribution in mountain streams should be obtained prior to dam construction. In this study, to identify the ideal structure for controlling debris flow, we evaluated the influence of different dam structures on capture rate. We also evaluated the relationship between grain size and capture rate for several different grain-size distributions in real mountain streambeds. The experimental results indicated that a vertical grid component strongly influences the capture rate and that a round cross-sectional structure exhibits half the capture rate of a square-shaped structure. Additionally, examination of the grain-size distribution of a real mountain stream indicated that grain-size distribution strongly influences capture rate.

Key words: capture rate, debris flow, experiment, grain size, steel-grid sabo dam.

1. INTRODUCTION

Debris flows in mountainous areas pose a threat to property and human well-being. Technologies such as steel-grid SABO dams are intended to mitigate these risks by controlling debris hazards in areas threatened by sediment flows. However, the exact mechanisms by which steel-grid SABO dams mitigate debris hazards is not fully understood, as reported by [*Hashimura et al*., 2012].

According to the design code of steel-grid SABO dams [*Japanese government*, 2007], the permeable width of the barricade must be the same size as the D_{95}, which is the particle diameter equivalent to 95% of the debris accumulation based on the frequency distribution of sediment sizes within a stream. Consequently, the permeable width of the barricade is determined not by considering particles under the 95% size distribution curve based on the grain-size accumulation rate (which is the relationship between the particle diameter and passage weight percentage). In contrast, the former SABO dam design code [*Japanese government*, 2000] ascribes the permeable width of the barricade as 1.5–2.0-fold that of the large particle diameter D_{95}. Hence, the width determined by the former design code [2000] is wider than that of the new code [2007]. For this design code transition, it is critical to determine the debris capture rate of steel-grid SABO dams to outline how well these dams control potentially damaging sediment flows.

The ways by which steel-grid SABO dams capture debris-flow sediment have been investigated previously [*Ashida et al*., 1987; *Mizuyama et al*., 1995; *Mizuno et al*., 2000; *Takahashi et al*., 2001]. [*Ashida et al*., 1987] proposed a probability model that predicts the sediment volume that flows out of the SABO dam grid. [*Mizuyama et al*., 1995] considered the relationship between SABO dam function and the characteristics of debris flow. [*Mizuno et al*., 2000] analyzed the movement of each particle using the distinct element method. [*Takahashi et al*., 2001] developed a numerical model that considers the momentary blockage-probability of a SABO dam. Additionally, [*Takahashi et al*., 2001] showed the relationship between the permeable width of the barricade and the coarse particle diameter using blockage mechanisms provided by the arch action of coarse particles, as shown in **Fig. 1**.

With reference to a steel structure, [*Yazawa et al*., 1986] proposed a new method to control debris flow using a steel grid constructed beneath a riverbed, which separates water from sediment in debris flowing through the grid. However, no study has reported the capture mechanisms of the grid SABO dam, with consideration to details pertaining to the capture rate, such as differences in the grid cross-section type or the incline of the barricade on the riverbed, or verified the applicability of the permeable width of the barricade determined by the SABO dam design code [*Japanese government*, 2000 & 2007].

To identify the ideal structure for controlling debris flow, the capture rate of a small grid dam in a laboratory flume was observed by varying several design parameters, such as the permeable width of the barricade, the type of cross section of the grid component, and the barricade incline on the riverbed. By calculating the capture rate under these conditions, the ideal permeable width of the barricade was determined by identifying the necessary volume concentration of particles (which determines the grid size) within a debris flow.

Finally, to evaluate the capture rate of a grid SABO dam designed according to code [2000], taking into consideration different particle size distributions, the grid size was altered according to the various particle size distribution curves.

2. IDEAL STRUCTURE OF A GRID SABO DAM FOR CONTROLLING SEDIMENT RUNOFF

To identify factors that affect the capture rate of a grid SABO dam, experiments were conducted in a laboratory flume with variation of several operational parameters.

2.1 Materials and Methods

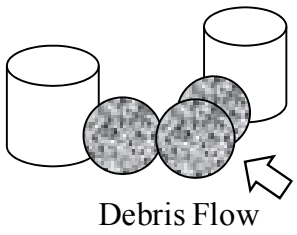

Fig. 1 Mechanisms of capture by the arch action of steel-grid SABO dams [*Takahashi et al*., 2001]

Fig. 2 shows the experimental flume apparatus. An experimental waterway, which had a height and width of 10 cm and a length of 100 cm, was constructed and a small-grid SABO dam barricade was incorporated at the downstream point.

Sediment with a particle diameter of ~7 mm (separated by sieving) was used to fill the waterway bed (deposition thickness t=15mm). Water containing stones was allowed to flow through the apparatus, emulating natural flows of sediment in water as would occur due to water movement. The weight of the particles captured by the barricade and the weight of the particles flowing out of the barricade were recorded. Various dam design parameters were altered to determine the impact on the capture rate, which is the relationship between the weight of grit blockaded by the obstacle grid and the weight of grit supplied from the upper point.

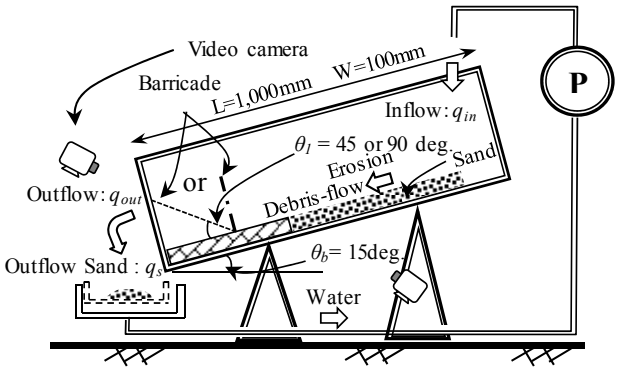

Fig. 2 Diagram of the experimental model

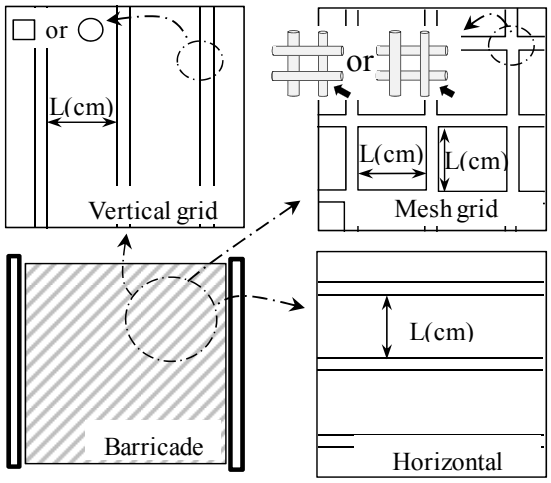

Fig. 3 Dam type (vertical grid, horizontal grid, or mesh grid) and cross-section type (square or circle) of the grid component used in the experimental case study

These parameters include the type of dam (vertical grid, horizontal grid, or mesh grid), as shown in **Fig. 3**; the cross-section type of the grid component (square or circle), as shown in **Fig. 3** (upper left); the permeable width of the barricade (grid size); the barricade incline on the riverbed, as shown in **Fig. 4**; and changing to a front-bar type of grid (where the vertical and horizontal components are arranged on the upstream, debris-flow side), as shown in **Fig. 3** (upper right). Finally, the effect on capture rate of the volume concentration of the sediment under debris flow (necessary sediment concentration for blockage by the barricade) was examined.

Table 1 shows the case study optimized by considering the performance parameters. θ_1 is the barricade incline on the riverbed, as shown in **Fig. 4**; L (*d) is the permeable width of the barricade (the ratio between the permeable width and the particle diameter d, where d = 7 mm); the dam type is the type of grid structure (vertical, horizontal, or mesh grid); the grill type is the type of cross section of the grid component (square or circle, upper left); the front-bar type is a grid component type for upstream (the difference between the vertical component and horizontal component arranged to the upstream, debris-flow side, upper right) (all shown in **Fig. 3**); V_L/V_S is the ratio between the coarse particle (V_L) and the fine particle (V_S) weights of the case study (from CASE 3-1 to CASE 3-12); and Q is the water discharge. Additionally, four particle diameters (d = approximately 1, 3.5, 7, & 10 mm) were used to fill the waterway bed at the same ratio (one-fourth) as in CASE 3-13.

The blockage of the small-grid SABO dam was recorded using video cameras. During this time, water was flowed continually for 3 seconds after blockage of the barricade to better understand the deformation of the deposit caused by erosion due to overtopping after the dam had become blocked with sediment.

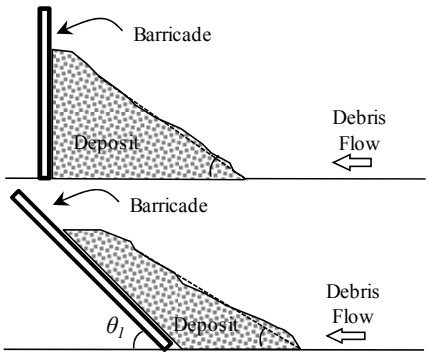

Fig. 4 Barricade incline used in the experimental case study

2.2 Ideal structure of grid SABO dam

The experiment was repeated three times under one condition, considering the inhomogeneity of the particle distribution under debris flow. **Table 2** shows the experimental results for the capture rate of the barricade. To clarify how the capture rate was affected by the design, **Figs. 5** to **10** show the difference between the measured capture rates, including each trial and the average capture rate, as well as the non-dimensional capture rate, which was normalized according to the maximum capture rate under the same design condition.

Table 1 Experimental case study

CASE	θ_1 (°)	L (*d)	Dam type	Grill type	Front-bar type	V_L/V_S (kg/kg)	Q (ℓ/s)
1-1	90	1.5	Gr.	□	Ver.	1.0/0.0	0.72
1-2					Hor.		
1-3				○	Ver.		
1-4			Hor.	□	-		
1-5			Ver.				
1-6				○			
1-7		2.0	Gr.		Ver.		
1-8			Ver.	□	-		
1-9			Hor.				
1-10			Ver.	○			
1-11		2.5	Gr.		Ver.		0.95
1-12		1.0					0.50
1-13		2.5					
1-14				□			
1-15		2.0			Hor.		0.72
2-1	45	1.5	Ver.		Ver.		
2-2					-		
2-3			Hor.				
2-4				○			
2-5		2.0	Gr.		Ver.		
2-6			Ver.		-		
2-7		1.0	Hor.				
2-8		1.5	Gr.		Ver.		
2-9	90	2.0					0.95
2-10	45	1.5	Hor.		-		
2-11							0.50
2-12	90	2.0	Gr.	□	Ver.	0.8/0.2	0.72
3-1							
3-2						0.6/0.4	
3-3						0.4/0.6	
3-4						0.2/0.8	
3-5						0.3/0.7	
3-6						0.5/0.5	
3-7							0.50
3-8							0.95
3-9	45	1.5					0.72
3-10		2.0					
3-11		1.5					0.95
3-12							0.50
3-13	90	2.0				Mix[*1]	0.72

*1: d ≒ 1, 3.5, 7, & 10 mm.
Gr.: Mesh grid, Hor.: Horizontal grid, Ver.: Vertical grid; □: Square, ○: Circle.

Table 2 Experimental results of capture rate (%)

CASE	1st	2nd	3rd	CASE	1st	2nd	3rd
1-1	96	96	96	2-6	0	0	0
1-2	94	94	96	2-7	96	95	95
1-3	96	96	96	2-8	6	2	4
1-4	82	86	86	2-9	88	88	88
1-5	92	90	90	2-10	8	38	8
1-6	90	90	94	2-11	76	88	82
1-7	90	86	90	2-12	94	94	94
1-8	72	74	82	3-1	74	74	72
1-9	0	0	0	3-2	58	70	60
1-10	24	52	32	3-3	50	0	34
1-11	38	36	42	3-4	0	0	0
1-12	96	96	98	3-5	0	0	0
1-13	62	58	44	3-6	60	58	60
1-14	4	30	16	3-7	60	60	56
1-15	56	54	62	3-8	52	56	54
2-1	94	94	96	3-9	62	48	60
2-2	80	44	82	3-10	6	16	16
2-3	62	74	58	3-11	52	46	56
2-4	10	70	22	3-12	68	58	68
2-5	90	90	76	3-13	61	54	63

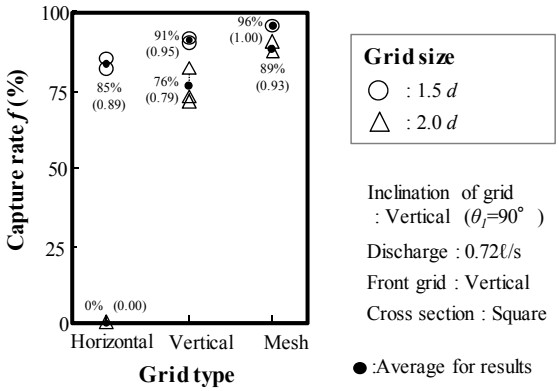

Fig. 5 Effect of grid type on capture rate (incline of dam = 90°)

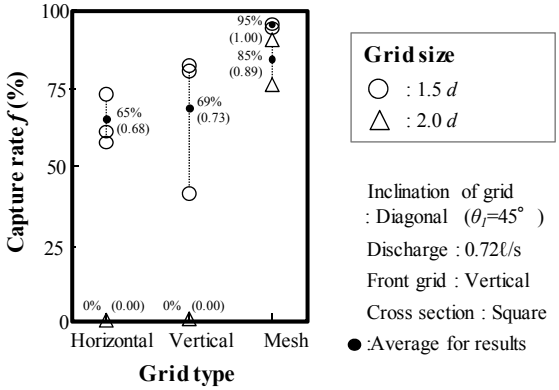

Fig. 6 Effect of grid type on capture rate (incline of dam = 45°)

Figs. 5 and **6** show the capture rate when the incline of the barricade was set to a 90° angle and a 45° angle to the riverbed, respectively, with various grid types.

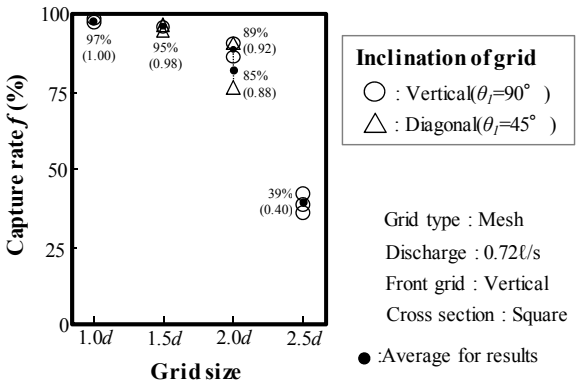

Fig. 7 Effect of the permeable width grid-size on capture rate (grid type = mesh grid)

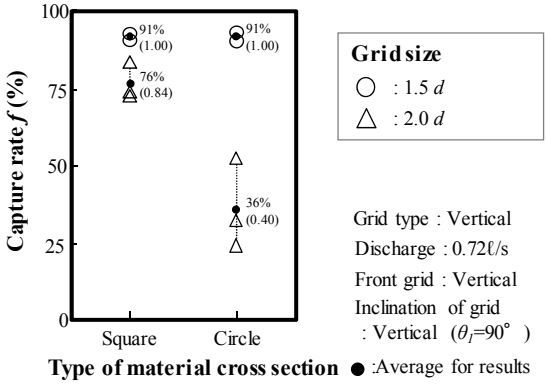

Fig. 8 Effect of grid cross section on capture rate

Dam design (shown in **Fig. 3**) did not affect capture rate, as shown in **Fig. 5**. In contrast, the experimental results suggested that the vertical component strongly contributed to blockage of the dam under the experimental conditions (with a grid size twofold larger than the particle diameter) when the horizontal component was absent, as shown in **Fig. 5**. This result suggested that the horizontal arch action by the vertical component strongly influenced the blockage mechanisms to compare with the vertical arch action by the horizontal component, as shown in **Fig. 1**. In terms of the effect of barricade incline on sediment capture, the vertically inclined barricade (θ_1 = 90°) captured more sediment particles than the diagonally inclined grid (θ_1 = 45°), as shown in **Figs. 5** and **6**; only the vertical and the horizontal component of the dam (non-mesh grid types; θ_1 = 45°) did not capture particles with a grid size twofold larger than the particle diameter, as shown in **Fig. 6**.

Fig. 7 shows the relationship between the permeable width of the barricade (mesh grid) and the capture rate. The capture rate was ~85% greater when the permeable width of the barricade was less than twofold the particle diameter, as shown in **Fig. 7**. In contrast, the capture rate was ~39% when the

permeable width of the barricade was 2.5-fold the particle diameter, as shown in **Fig. 7**.

Fig. 8 shows the relationship between the capture rate and the grid-component cross section. The cross section did not affect the capture rate when the permeable width of the barricade was less than 1.5-fold the particle diameter, as shown in **Fig. 8**. However, the square cross section captured twofold more material than the circular cross section, possibly because particles center on the square component more easily without slipping, as shown in **Fig. 1**, allowing an arch of particles to form rapidly. This promoted rapid blockage, which contributed to the high capture rate.

Fig. 9 shows the relationship between discharge and the capture rate. No effect of discharge on capture rate was found when the permeable width of the barricade was twofold the coarse particle diameter, as shown in **Fig. 9.** However, the capture rate did decrease in response to an increase in flow. This occurs because almost all of the particles are initially captured by the barricade when the permeable width of the barricade is less than twofold the particle diameter, but a proportion of the captured particles is then eroded when the flow overtops the dam. Erosion due to the overtopping causes a decrease in the capture rate. In contrast, the capture rate increases in response to an increase in flow when the permeable width of the barricade is 2.5-fold the particle diameter. To explain this, it is assumed that the flow velocity (including water and particles) increases due to the increase in flow. The increase in the particle-flow velocity then affects the early blockage, as shown in **Fig. 1**. Finally, the volume of particles flowing through the barricade decreases upon deposition. Future work is needed to verify the relationship between capture rate and flow velocity.

Fig. 10 shows the relationship between capture rate and the mesh grid component oriented upstream, as shown in **Fig. 3** (upper right).

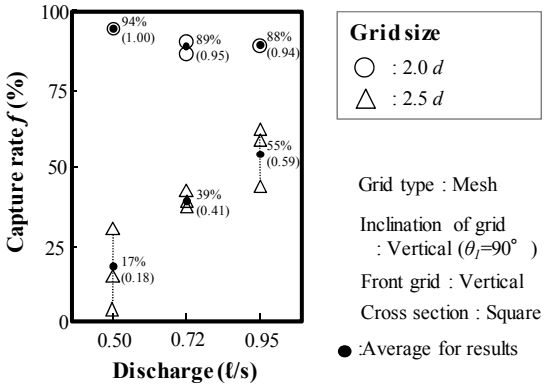

Fig. 9 Effect of water discharge on capture rate

No effect on capture rate was observed when the permeable width of the barricade was 1.5-fold the particle diameter, as shown in **Fig. 10**. However, the use of a front-bar type grid in vertical orientation toward the upstream direction demonstrated a capture rate ~1.5-fold that of the horizontal orientation when the permeable width of the barricade was twofold the particle diameter.

These results (**Figs. 5** to **10**) indicate the ideal structure of the grid SABO dam, as shown in **Fig. 11**. This configuration assumes that it is difficult to remove captured particles from the square grid; thus, this study proposes that a trapezoid grid would make maintenance simpler and removal of particles easier compared to a square grid.

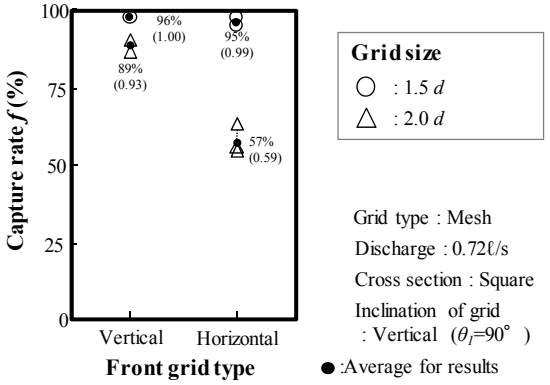

Fig. 10 Effect of front-bar-type mesh grid on capture rate

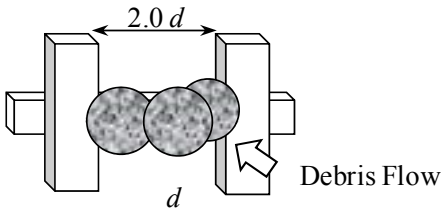

Fig. 11 Schematic of an ideal-grid SABO dam based on the experimental results

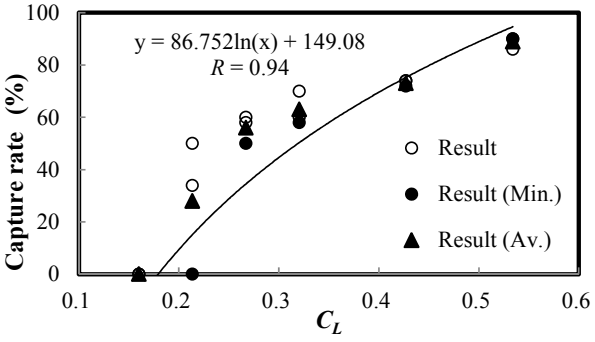

Fig. 12 Relationship between capture rate and volume concentration of coarse particles in debris flow (grid size is twofold the coarse particle diameter)

Experiments were conducted for cases 3-1 to 3-12, a scenario that involves two particle diameters (d = 3.5 & 7 mm), and CASE 3-13, which uses four particle diameters (d = 1, 3.5, 7, & 10 mm), as shown in **Table 1**. **Fig. 12** shows the relationship between the capture rate and the volume concentration of coarse particles (more than d = 7 mm) under debris flow. As shown in **Fig. 12**, the x-axis represents the volume concentration C_L of coarse particles within the debris flow, and the y-axis is the capture rate when the permeable width of the barricade is twofold the coarse particle diameter; discharge did not affect capture rate when the permeable width of the barricade was twofold the particle diameter, as shown in **Fig. 9**. **Fig. 12** shows the regression line of each capture rate in cases 3-1 to 3-12 using each minimum capture rate.

The correlation coefficient using the regression coefficient R was 0.94, as shown in **Fig. 12**. However, **Fig. 12** did not consider the effects caused by experimental conditions. Future work is needed to verify the regression coefficient. Assuming that the minimum capture rate necessary to achieve blockage is 70% (the ideal capture rate in this paper), the necessary volume concentration C_L of coarse particles is more than 0.4 (40%), as shown in **Fig. 12**.

3. EVALUATING CAPTURE RATE VERSUS GRAIN-SIZE DISTRIBUTION IN A REAL MOUNTAIN STREAMBED

To understand how capture rate is affected by the particle diameter distribution, one first requires an understanding of the grain-size distribution encountered in the field, assuming that a connection can be established between laboratory experiments and real-world functioning of this technology.

3.1 Examination conditions

Fig. 13 shows the four distribution curves of grain-size frequency under examination: three distribution curves (Torrents A, B, & C) were investigated in mountain streambeds, and one distribution curve (Test case) was assumed in order to understand how capture rate is affected by the grain-size distribution.

Fig. 14 shows the grain-size accumulation rate, which is the relationship between the particle diameter and the passage weight percentage using the grain-size frequency shown in **Fig. 13**, assuming the same distribution as in **Figs. 13** and **14**, to determine the effect of the grain-size distribution using the volume concentration of coarse particles in sediment runoff.

Previously, it was assumed that the riverbed incline around the dam is constant, that the incline does not change due to debris deposition on the riverbed, and that the volume concentration of coarse particles under debris flow is constant (C_{max} = 0.54: C_{max} = $0.9C_*$, C_* is equal to the volume concentration of the bed particles 0.6, [*Japanese government, 2007*]). Additionally, the interstitial particle density was assumed to be constant.

3.2 Relationship between the permeable width of the barricade and grain-size distribution

Table 3 shows the permeable width of the barricade as determined by the SABO dam design code [2000 & 2007] using the grain-size distributions (Torrents A, B, C & Test case) shown in **Fig. 14**. Specifically, the permeable width of the barricade is 1.0- or 1.5-fold the coarse particle diameter (D_{95}), which was determined using **Fig. 13**. The volume concentration of coarse particles (C_L = 0.4) necessary to cause blockage was divided by the volume concentration of all particles (C_{max} = 0.54).

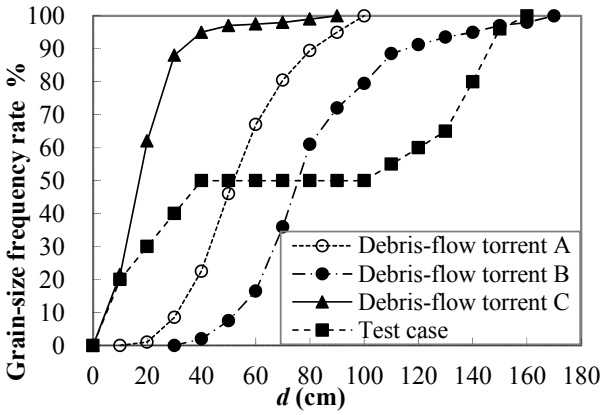

Fig. 13 Distribution curves of grain-size frequency

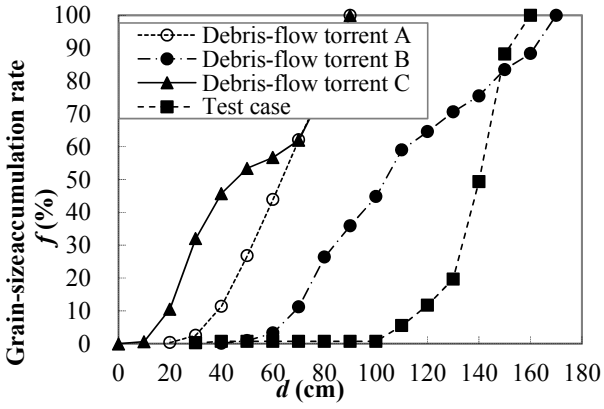

Fig. 14 Grain-size distribution curve (relationship between particle diameter and grain-size accumulation rate: passage weight percentage)

Table 3. Permeable width of the barricade according to the [2000] & [2007] design codes and capture rate (%) of a grid planned according to the [2000] design code ($1.5D_{95}$)

	$1.5D_{95}$ (cm)	$1.0D_{95}$ (cm)	$2.0D_{CL}$ (cm)	Capture rate :$1.5D_{95}$ (%)
Torrent A	120	80	90	52
Torrent B	210	140	150	41
Torrent C	60	40	50	63
Test case	210	140	270	78

Table 3 shows an ideal grid for blockage of $2.0D_{CL}$, which is twofold the particle diameter d considering the coarse particle existence rate f_{bL} = 26%, where $f_{bL} = (1 - C_L/C_{max})\cdot 100$. The new width D_{cL} was determined by the grain-size distribution curves, as shown in **Fig. 14**, using the calculated existence rate f_{bL} of coarse particles in the total particles.

This permeable width of $2.0D_{cL}$ is ideal when the grain-size distribution is considered. The permeable width of $2.0D_{cL}$ lies between the width determined by the [2000] design code ($1.5D_{95}$) and that of the [2007] code ($1.0D_{95}$) for real mountain streams (Torrents A, B, & C). In contrast, in the test case, the permeable width of $2.0D_{cL}$ is wider than those determined by the old and new design codes. Hence, it is necessary to consider the grain-size distribution prior to the construction of a new SABO dam.

To understand the capture rate of a barricade with a permeable width of $1.5D_{95}$, as determined by the [2000] design code for mountain streambeds, the existence rate of the coarse particle fraction was calculated using the grain-size distribution, as shown in **Fig. 14**. Finally, the volume concentration of coarse particles within the debris flow C_L was calculated by multiplying the existence rate of coarse particles f_{bL} by the volume concentration of all particles (where C_{max} = 0.54). **Table 3** shows the capture rate ($1.5D_{95}$) for the mountain streambeds (Torrents A, B, & C) shown in **Fig. 14**, using both the volume concentration of coarse particles within debris flow C_L and the relationship between the capture rate and the volume concentration of coarse particles, as shown in **Fig. 12**. The barricade capture rate changed with grain-size distribution; mountain streambeds (Torrents A, B, & C) demonstrated a difference of a 1.5-fold greater capture rate, as shown in **Table 3**. Additionally, the capture rate of the grid SABO dam built according to the specifications of the [2000] design code was less than 70% (*i.e.*, 41–63%).

This work assumes that the volume concentration of particles within a debris flow is constant.

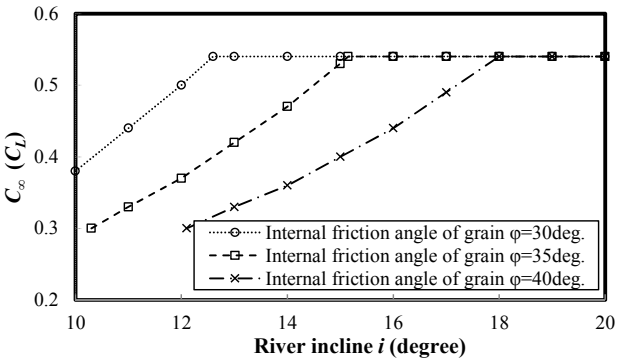

Fig. 15 Relationship between riverbed incline and volume concentration of particles

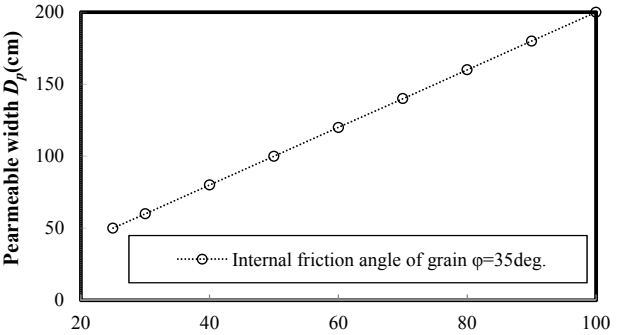

Fig. 16 Relationship between permeable width of barricade and grain-size distribution curve

However, when the riverbed around a grid SABO dam is on a gradual incline or on flat ground, coarse particles separate from the debris flow, deposit on the riverbed, and cannot flow to the barricade. Hence, the barricade cannot capture the fine particles due to the lack of formation of a blockade. Thus, the capture rate was examined by considering the relationship between capture rate and riverbed incline around the upstream area of the dam.

Using the relationship between the riverbed incline and the volume concentration of particles within the debris flow [*Japanese government,* 2007], the equilibrium concentration C_∞ at the point is expressed as:

$$C_\infty = \frac{\rho \tan\theta_w}{(\sigma - \rho)(\tan\phi - \tan\theta_w)} \qquad (1)$$

where ρ is the interstitial fluid, σ is the density of the particle, ϕ is the internal friction angle of grit, and θ_w is the riverbed incline at the point. Assuming that the volume concentration of coarse particles within the debris flow C_L equals the equilibrium

concentration C_∞ at the point in question, **Fig. 15** shows the relationship between riverbed incline and the volume concentration of particles C_∞ (=C_L) according to Eq. (1), where the volume concentration of the coarse particles C_L is assumed to be 0.54 (C_{max}), per the [2007] design code. To capture more than 70% of the sediment flow using the barricade, the volume concentration of coarse particles in the sediment runoff must be more than 40%, as shown in **Fig. 12**. Additionally, when the internal friction angle of the particle is 35°, the suggested riverbed angle must be greater than 13°, as shown in **Fig. 15**.

Fig. 16 shows the relationship between grain size determined by distribution curve and the ideal permeable width of the barricade under varying incline conditions (13–15°). The internal friction angle of grit is assumed to be 35°, and the depth of debris flow is greater than the particle diameter.

The coarse particle existence rate within all particle in the debris flow f, where $f = (1.0 - C_L/C) \cdot 100$, is 5% when the volume concentration of the coarse particles (C_L=0.4, C=0.42: ρ=1,200kg/m^3, σ=2,600kg/m^3, ϕ=35°, θ_w=13°) necessary to blockade the barricade is divided by the volume concentration of particles on the riverbed incline (13°), as shown in **Fig. 15**. Additionally, the particle existence rate of the necessary volume concentrations of particles on riverbed inclines of 14° and 15° are 15% and 25%, respectively. The grain size $d_{f5\text{-}25}$ is calculated with the above coarse particle rate f using the grain-size distribution curve (*e.g.*, **Fig. 14**). Furthermore, the relationship between the permeable width of the barricade and the grain size $d_{f5\text{-}25}$, shown in **Fig. 16**, can be used to describe the functioning of grid SABO dams. However, in the future, grain coarsening in debris flows needs to be considered in order to identify the exact performance mechanisms of steel-grid SABO dams.

4. SUMMARY

To identify the ideal structure for controlling sediment runoff, this study examined multiple grid SABO dam design parameters and determined how capture rate is affected by different configurations. Additionally, the functionality of SABO dams constructed under different design codes was examined.

This work showed that the vertical component of the dam grid is critical for blocking sediment, whereas the horizontal component is less important. Considering the relationship between the permeable width of the barricade and capture rate, this suggests that the necessary permeable width of the barricade is less than approximately twofold the coarse particle size (2.0d). Additionally, these results showed when considering capture rate that a square grid retains more sediment than a round grid. Furthermore, the vertical incline of the barricade, when compared to the riverbed and the mesh grid vertical component oriented toward the upstream direction, is important in terms of optimizing capture rate. Assuming that these laboratory experiments are directly applicable to the field, the volume concentration of coarse particles should be greater than 0.4 (capture rate = more than 70%), and the permeable width of the barricade should be twofold the coarse particle diameter.

This study, which took into consideration the grain-size distribution in a mountain streambed, showed that capture rate was affected markedly by the grain-size distribution. In terms of riverbed characteristics, the incline of the riverbed upstream of a dam must be greater than 13° to block more than 70% of sediment. This work also suggests that the ideal permeable width of the barricade under different incline conditions (13, 14, & 15°) should be determined with consideration of the grain-size distribution. Future work is needed to consider the effect caused by experimental conditions.

REFERENCES

Ashida, K., Egashira, S., Kurita, M & Aramaki, H. (1987): Debris flow controlled by grid dams. Disaster Prevention Research Institute Annuals for Kyoto University, Vol. 30, pp. 441-456.

Hashimura. K., Hashimoto, H., Miyoshi, T., Ikematu, S,. Hasuo S,. Farouka M, & Sakata, K. (2012): Flume experiment for capture ability of wood, stone and water by grid SABO dam. Annual research presentation meeting. Japan Society of Erosion Control Engineering, pp. 72-73.

Ministry of Construction, Japan, 2000: Manual of Technical Standard for designing Sabo facilities against debris flow

Ministry of Land, Infrastructure, Transport and Tourism, Japan, 2007: Manual of Technical Standard for designing Sabo facilities against debris flow and driftwood

Mizuno, H., Mizuyama, T., Minami, T. & Kuraoka, C. pp. 2000. Analysis of simulating debris flow captured by permeable type dam using Distinct Element Method. Journal archive/sabo, Vol. 52/ No.6, pp. 4-11.

Mizuyama, T., Kobashi, S. & Mizuno, H. (1995): Control of passing sediment with grid-type dams, Journal archive. sabo, Vol. 47, No.5, pp. 8-13.

National Institute for Land and Infrastructure Management Ministry of Land, Japan (2007): Manual of Technical Standard for designing Sabo facilities against debris flow and driftwood.

Takahashi, T., Nakagawa, H., Satofuka, Y. & Wang, H. (2001): Stochastic model of blocking for a grid-type dam by large boulders in a debris flow, Annual Journal of Hydro science and Hydraulic Engineering, Vol. 45, pp. 697-702.

Yazawa, A., Mizuyama, T. & Morita, A. (1986): Experiments and analysis on Debris Flow Braker screen. Memorandum of PWRI, Vol. 2374.